https://doi.org/10.46813/2023-147-015

FEATURES OF MODIFICATIONS IN RE-SOLIDIFIED SURFACES OF ADVANCED MATERIALS DUE TO HIGH-POWER PLASMA PULSES

S.S. Herashchenko[1], V.A. Makhlai[1,2], I.E. Garkusha[1,2], Yu.V. Petrov[1], N.N. Aksenov[1], N.V. Kulik[1], D.V. Yelisyeyev[1], P.B. Shevchuk[1], Y.E. Volkova[1,2], T.M. Merenkova[1], M. Wirtz[3]
[1]Institute of Plasma Physics, National Science Center "Kharkov Institute of Physics and Technology", Kharkiv, Ukraine;
[2]V.N. Karazin Kharkiv National University, Kharkiv, Ukraine;
[3]Forschungszentrum Jülich GmbH, Institut für Energie- und Klimaforschung, Jülich, Germany
E-mail: gerashchenko@kipt.kharkov.ua

The surface modification of advanced materials was studied through a series of repetitive plasma pulses caused tungsten melting. Features of the affected surface layers in reference materials (IGP W, AM W/WTa, Hastelloy, and EUROFER) for both fusion and fission applications were explored after exposure to plasma in the facilities (QSPA, MPC, and PPA) with different durations of plasma pulses. A detailed surface analysis was carried out with Scanning Electron Microscopy. It was found that the plasma treatment led to the formation of a modified layer as a result of the rapid re-solidification of the exposed surface. The fine cellular structures appeared in the re-solidified layers of the irradiated materials, with typical cell sizes ranging from 150 to 500 nm. An increase in the roughness of the exposed surfaces was attributed to the presence of the cracks and re-solidified layer.

PACS: 52.40.Hf; 52.70

INTRODUCTION

Advanced high-performance materials used in nuclear power reactors, both for fission and fusion applications, must endure severe conditions such as high heat loads, particle bombardments, high-energy neutron irradiation, etc. [1, 2]. A comprehensive understanding of the mechanisms behind materials damage effects and dedicated efforts toward mitigation will yield substantial benefits that apply across various nuclear environments.

Tungsten is a primary material that will be used as a first-wall and a divertor armour in fusion devices like ITER and DEMO due to its high melting point, high thermal conductivity, low sputtering yield, and tritium retention [3, 4]. The development of advanced tungsten products made using various production/densification technologies, i.e., forging and rolling, additive manufacturing (AM), W-based alloys, W-composites, and W-fibres requires thorough testing and characterization under harsh fusion-relevant conditions (including H isotopes, He, etc) [1, 3, 5–7].

Hastelloy and other nickel alloys are designed for effective performance under high-temperature, high-stress conditions, particularly in situations where conventional and less ex
pensive iron-based alloys (steels) would not be suitable. Hastelloy is commonly used as construction material for pressure vessels in power reactors and valves in the chemical industry, among other applications [8].

Reduced Activation Ferritic Martensitic (RAFM) steels, such as EUROFER, are relevant structural materials used in fission and future fusion power plants [9–11]. This choice is due to their high resistance to swelling and low rates of irradiation-induced creep, which refers to the slow changes in dimensions of materials exposed to prolonged stresses caused by X-rays, γ-rays, and n-irradiation, etc).

Pulsed plasma facilities encompass a range of scenarios involving high heat and particle loads onto the surfaces. These facilities are used to make surface modifications [11, 12] for various technologies, study erosion mechanisms of different materials, and uncover the risks associated with plasma contamination by erosion products.

Previous research has revealed the key mechanisms governing tungsten erosion under transient loads. These include the formation of a melt layer, the development of instabilities within this layer, and the emergence of progressive corrugations, all of which contribute significantly to material damage [13–18]. Additionally, the cracking thresholds were evaluated for various tungsten materials, considering the number of pulses and the initial temperature of the samples under investigation. Furthermore, the presence of micropores and blisters on the exposed surfaces was also observed [19].

Special mention should be made of the process of high-cycle re-solidification in metals under conditions of rapid surface heating and melting. This process induces surface modifications that result in increased microhardness and durability [12]. In experiments [14–18], the cellular structures were observed on the exposed surfaces. It was shown that the cellular structures can have a significant influence on the mechanical and thermal properties of the solidified metal [20–24]. The size and distribution of cells can impact the material strength, ductility, and thermal conductivity. The features and their effects on material stability and resilience under extreme plasma heat loads require further investigations.

This work is devoted to the characterization of surface modifications originated during a solidification process in materials under various plasma stream conditions, i.e., different pulse duration, plasma species, and applied heat loads.

1. EXPERIMENTAL FACILITIES, SAMPLES AND DIAGNOSTICS

Samples of pure IGP tungsten with the transversal (T) grain orientation and in the recrystallized (R) state were used for the experiments (Figs. 1 and 2) [4, 18, 25]. Samples had sizes of 12×12×5 mm. All specimens were polished to achieve a mirror-like surface. The samples were supplied by Plansee AG, prepared and delivered from Forschungszentrum Julich.

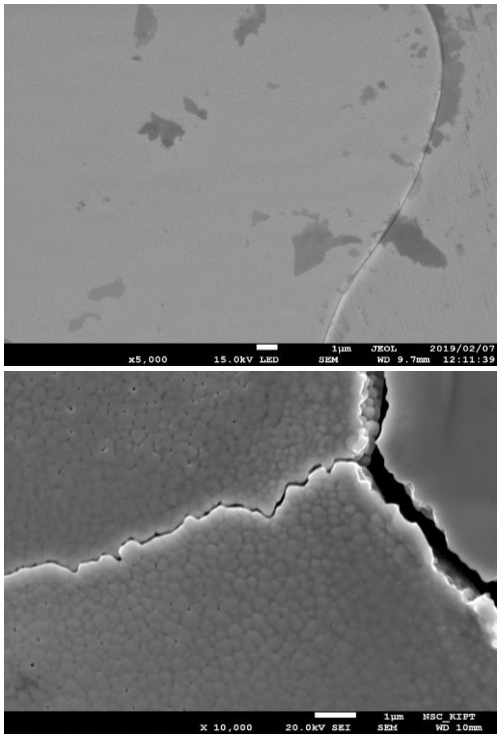

a

b

Fig. 1. SEM images at various magnifications of IGP tungsten recrystalized sample: a – in as-received state; b – exposed to the hydrogen QSPA plasma, T_{base} = 400 °C. Scale bar – 1 μm

Two types of samples, which were produced using AM based on the laser powder bed fusion (LPBF) method, were also tested (Figs. 3 and 4) [3, 5]. Advanced materials were fabricated at Fraunhofer Augsburg (under the direction of IPP Garching) [3] and Renishaw PLC (under the direction of CCFE) [5]. The size of powder particles was 10...50 μm. These materials took the form of nominal 1 cm cubes of lattice material in both pure W and W-6% Ta, with a range of lattice parameters designed by Uni Tuscia.

A sample of Hastelloy N (Fig. 5), a Ni-based superalloy, was subjected to plasma irradiation, along with other alloying elements such as Mo, Cr, Fe, Si, and Mn in varying percentages.

Samples of EUROFER steel (Cr-9.7%, Mn-0.7%, W-0.8%, Fe-89.6%) [9, 10] were also utilized in the reported experiments (Fig. 6). The samples had dimensions of 15×12×1 mm, and all specimens were mechanically polished to achieve a mirror-like surface.

The study of surface modifications under the high-power pulsed plasma streams was performed using three different facilities: QSPA Kh-50, MPC, and PPA.

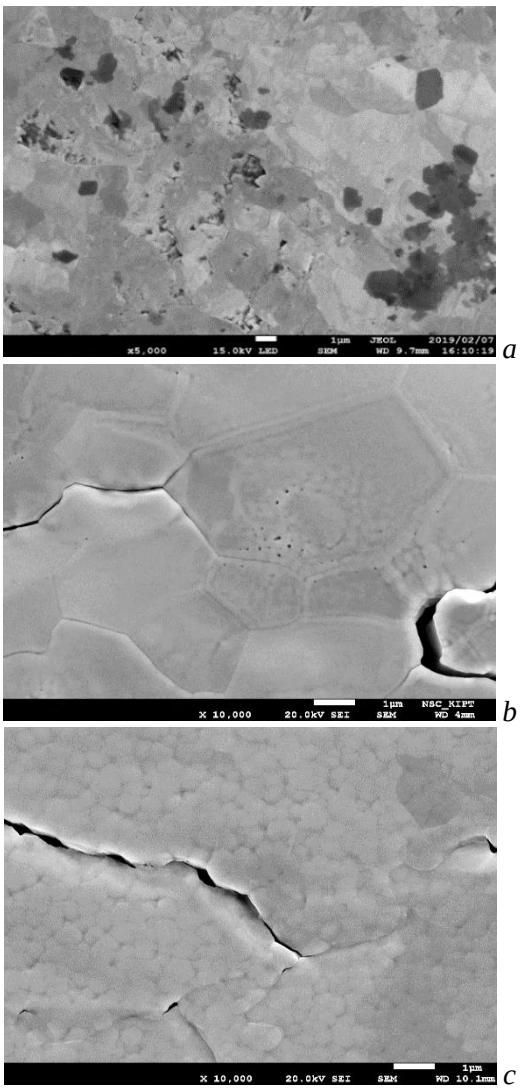

a

b

c

Fig. 2. SEM images at various magnifications of IGP tungsten transversal sample: a – in as-received state; b – exposed to the hydrogen QSPA plasma, T_{base} = 400 °C; c – exposed to the short-pulse helium plasma of MPC, T_{base} = RT. Scale bar – 1 μm

The large-scale QSPA Kh-50 device [13–18, 26, 29] reproduced the fusion reactors transient conditions. The main parameters of the QSPA hydrogen plasma streams included an ion impact energy of about 0.4 keV, a maximum plasma pressure of 0.32 MPa (higher than the plasma pressure relevant to fusion reactors), and a stream diameter of 18 cm. The plasma pulse shape was approximately triangular with a pulse duration of 0.25 ms. The plasma stream energy density was up to 3 MJ/m^2. The samples were preheated to the required initial temperatures (T_{base}) using a special heater [26] before and between plasma pulses.

The MPC facility [11, 27] generated helium compressed plasma streams with a plasma density (n_e) around 10^{18} cm^{-3}, and a plasma energy density ranging from 0.05 to 0.5 MJ/m^2. The discharge half-period was equal to about 10 μs. The experiments were carried out using pure helium at an initial pressure of 266.64 Pa.

The pulsed plasma accelerator, PPA [28], generated nitrogen plasma streams with ion energies of 350 eV and a plasma density of $(2…20)\cdot10^{14}$ cm^{-3}. Plasma energy density varied in the range from 0.05 to

0.4 MJ/m^2 and the plasma stream duration amounted to about 5 μs.

The heat loads onto the exposed surfaces were selected to operate above the melting threshold of the treated materials [15–18, 27, 28].

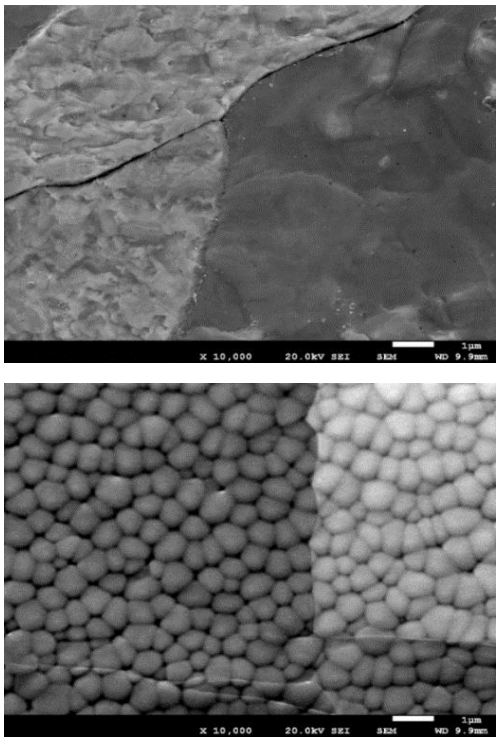

Fig. 3. SEM images at various magnifications of polished AM W sample: a – in as-received state; b – exposed to the hydrogen QSPA plasma, T_{base} = 600 °C. Scale bar – 1 μm

The ion source DSM-2 [29] was used for sputtering of some samples. An ion source was the system based on a microwave discharge in hydrogen within a mirror magnetic trap, which was operated at the electron cyclotron resonance (ECR) frequency of 2.37 GHz. The plasma density (n_e) in this system was about 10^{10} cm^{-3}, and the electron temperature T_e reached about 5 eV. The plasma ions were accelerated by applying a negative potential (-200 V) to the water-cooled holder. The base temperature of a sample during ion beam exposure was controlled by adjusting the cooling rate of the sample holder.

The microstructure was examined using SEM (JSM 7001F) equipped with an energy-dispersive X-ray analysis system (EDXA, Inca Energy-350). Mass measurements were performed during the experiment to monitor the mass loss (ΔM) with an accuracy of ±15 μg.

2. ADVANCED TUNGSTEN MATERIALS UNDER HIGH-POWER PULSED PLASMA LOADS

The samples of IGP tungsten (see Figs. 1,a; 2,a) were exposed to QSPA Kh-50 plasma with the surface heat load of 0.75 MJ/m^2 and T_{base} = 400 °C during an experimental series consisting of 200 pulses [18]. The affected surfaces were characterized by the formation of melted and consequently re-solidified layer and networks of intergranular cracks [18]. The width of such cracks reached up to several μm.

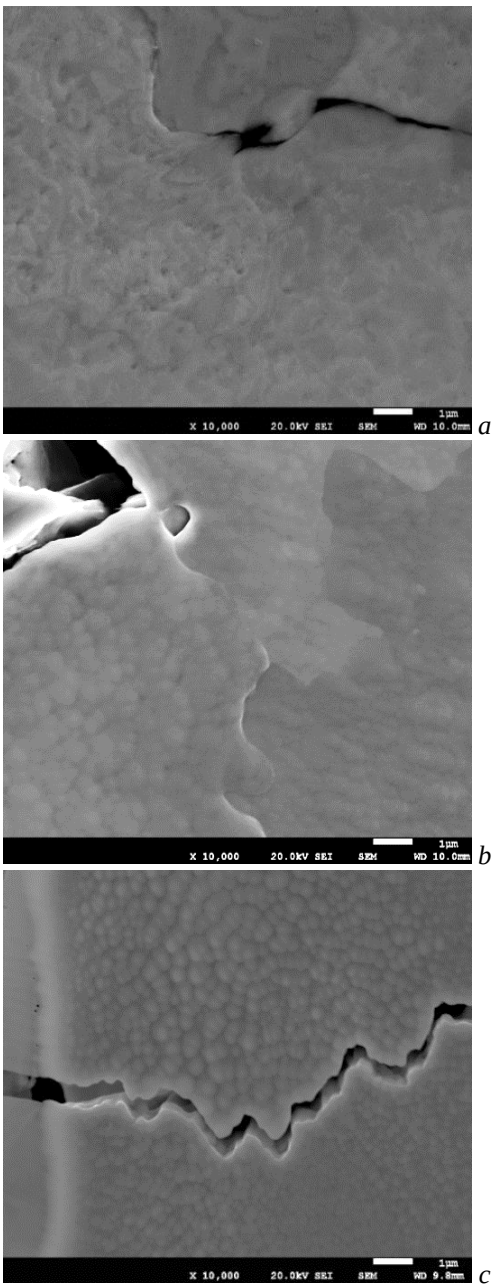

Fig. 4. SEM images at various magnifications of polished AM WTa sample: a – in as-received state; b – exposed to the hydrogen QSPA plasma, T_{base} = 600 °C; c – exposed to short-pulse helium plasma of MPC, T_{base} = RT. Scale bar – 1 μm

A corrugated structure was also formed on exposed surfaces as a result of repetitive plasma impacts. Moreover, the exposed surface of the R sample showed the presence of the fine cellular structure with a typical cell size of 150…250 nm (see Fig. 1,b). At this time, SEM images of surface modification of the T sample revealed only small clusters of the cellular structures that are isolated from each other (see Fig. 2,b).

It should be noted that after 10 plasma pulses with the surface heat load of 0.4 MJ/m^2 in the MPC facility at an initial temperature, T_{base} = RT, the cellular structure with the cell sizes ranging from 150 to 400 nm appeared on the surface of the T sample (see Fig. 2,c).

The perspective AM W (see Fig. 3,a) and AM WTa (see Fig. 4,a) materials were tested under 5 pulses of

QSPA Kh-50 plasma, with initial temperature, T_{base}, maintained at 500 ºC [3, 5]. The surface heat load, as measured with a calorimeter, achieved a level of 1.1 MJ/m^2. The surface analysis of the exposed samples revealed the presence of the re-solidified layer, cracks, pores, and balls [5]. Finally, the fine cellular structures were observed on the surface of all samples, with typical cell sizes of 150…500 nm (see Figs. 3,b; 4,b).

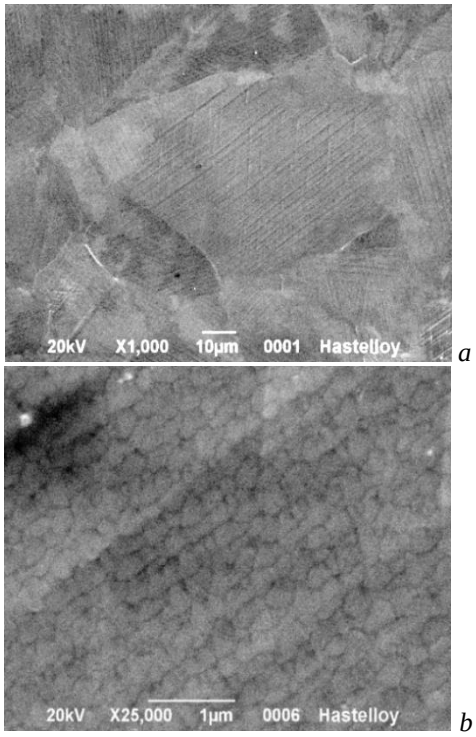

Fig. 5. SEM images at various magnifications of Hastelloy N sample exposed to short-pulse nitrogen plasma of PPA. T_{base} = RT. Scale bars: 10 µm (a); 1 µm (b)

Furthermore, the latticed sample of AM WTa was damaged by 10 pulses of MPC plasma with the surface heat load of 0.4 MJ/m^2 at an initial temperature, T_{base} = RT. Similar to the exposure in the QSPA, the cellular structure with cell sizes ranging from 150 to 500 nm occurred on the surface (see Fig. 4,c).

3. SURFACE MODIFICATIONS OF HASTELLOY AND EUROFER ALLOYS

A modified surface layer with an essentially changed structure has been formed in Hastelloy samples as a result of exposure to 5 plasma pulses in the PPA facility, with the surface heat load of 0.3 MJ/m^2 (Fig. 5) at an initial temperature, T_{base} = RT. Fig. 5,a demonstrates typical "large-scale" grain structures with grain sizes up to 50…100 µm and the absence of the cracks or other visual macro-defects. Nevertheless, Fig. 5,b at higher magnification reveals that short-pulse plasma of PPA caused the development of the cellular structures with submicron- and nano-dimension. In particular, the typical cell sizes are 200…500 nm. Furthermore, it is worth mentioning that these ordered cellular surface structures are primarily oriented along the direction of surface machining, which was previously applied for sample surface preparation.

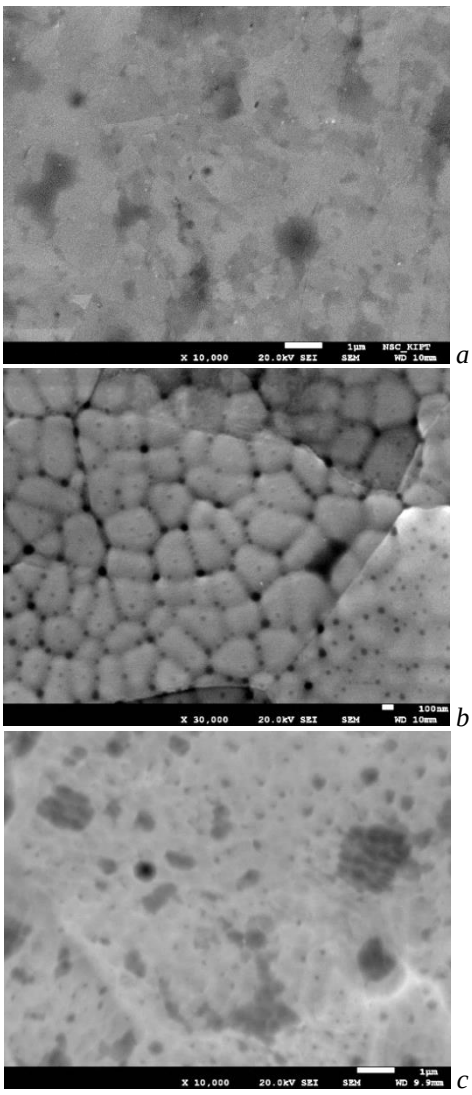

Fig. 6. SEM images at various magnifications of EUROFER sample: a – in as-received state; b – exposed to the QSPA plasma; c – exposed to the QSPA plasma and consequent H-ion beam. T_{base} = 200 °C. Scale bars: 1 µm (a, c), 100 nm (b)

The EUROFER sample (Fig. 6,a) was exposed to consequent pulsed and steady-state plasma irradiation. In particular, the QSPA performed the impact of 10 plasma pulses of 0.6 MJ/m^2. DSM-2 facility was used to provide the H-ion beam bombardment under normal incidence of the pre-damaged sample to an equivalent QSPA fluence of $2.4 \cdot 10^{24}$ m^{-2}. For that reason, the sputtering procedure was carried out over a duration of 5 h with a current density of 2.1671 mA·cm^{-2}. The initial temperature, T_{base}, of the samples during the exposures was 180 ºC.

Pulsed plasma loads resulted in changes in the surface microstructure of the exposed sample. The surface analysis reveals the pronounced sputter erosion morphology and an increased roughness due to the difference in height among grains. In addition, SEM images show the presence of the pores and cellular structures in the re-solidified layer of affected EUROFER. The typical sizes of the observed cells were 150…400 nm.

The steady-state irradiation of the sample caused the development of the surface relief typical for physical

sputtering. Traces of the cellular structures have not been observed.

The sample was weighted both before and after the sputtering procedure. The measured mass loss (Δm) achieved 415 μg.

4. DISCUSSION AND CONCLUSIONS

Pulsed plasma exposures led to the surface modifications of samples made from various materials. Applied plasma loads caused the development of the re-solidified layers and cellular structures on the exposed surfaces.

The cellular structures on the solidified metal surfaces due to thermocapillary (Benard-Marangoni) convection caused by surface tension gradient are a distinctive and often visually striking pattern of surface morphology [20–24]. This phenomenon occurs during the cooling and solidification of molten metals or alloys when Benard-Marangoni convection influences the flow and distribution of material on the surface. The material is transported from the regions of lower surface tension (warmer areas) to the regions of higher surface tension (cooler areas). Therefore, it accumulates and solidifies in certain regions, forming cells. These cells have distinct boundaries and often exhibit a hexagonal or polygonal shape [20–24] and tend to align along the direction of the temperature gradient. This process could be influenced by the concentration of surface-active elements or impurities.

In our experiments, the highest temperature gradient of ~ 10^8 K·m^{-1} develops across the liquid-solid interface, followed by the rapid solidification of material due to one plasma impact. The ultrafast cooling rates of ~ 10^6…10^7 K·s^{-1} are achieved driven by the contact of the thin melt layer and the massive bulk of the sample. Therefore, the solidification rate is ~ 10^{-2} m/s.

The sizes of observed cells reached 150…500 nm, slightly depending on the material and used plasma species.

The depth of the sputtered layer (d) of the EUROFER sample, assuming Fe as its material, derived from weight-loss measurements, dm, (area of the sample, $S = 1.8 \cdot 10^{-4}$ m^2) is $d \approx 300$ nm. The depth of molten Fe under QSPA pulse is $h_{melt} \approx 30$ μm [11]. Therefore, the depth of the cellular sub-grain structure, $h \leq d << h_{melt}$, and h is close to the observed size of the cells on the exposed surface. The obtained results are in agreement with the experimental data from [20–24].

Finally, the sub-grain patterns probably were created by Bénard-Marangoni instability superimposed on the macro-grain solidification that is determined by the parameters of the temperature gradient and solidification rate [20–24].

The surface modifications resulting from the solidification process in various materials were characterized in the experiments conducted at QSPA, MPC, and PPA, involving different plasma stream conditions, such as varying pulse duration, plasma species, and applied heat loads.

The plasma impacts led to the formation of the re-solidified layers on the exposed surfaces, accompanied by the presence of the cracks, progressive corrugations, pores, and spheres observed on the irradiated surfaces.

The fine cellular structure with the typical cell size of 150…500 nm appeared in the re-solidified layer for materials including IGP W, AM W/Ta, Hastelloy, and EUROFER samples.

A submicron-sized cellular sub-grain structure on the exposed surfaces can be attributed to the high-temperature gradient within the molten layer, influenced by the Bénard-Marangoni instability superimposed on the macro-grain solidification process.

ACKNOWLEDGEMENTS

This work has been carried out within the framework of the EUROfusion Consortium, funded by the European Union via the Euratom Research and Training Programme (Grant Agreement №101052200 – EUROfusion). Views and opinions expressed are however those of the author(s) only and do not necessarily reflect those of the European Union or the European Commission. Neither the European Union nor the European Commission can be held responsible for them. Work performed under EUROfusion WP PWIE and WP MAT.

This work has been supported by the National Academy of Sciences of Ukraine within the projects 22X-02-04/2023, 59-08/06-2023. This work was supported in part by the Ministry of Education and Science of Ukraine within the joint Ukraine-Austria research project (UA 10/2023). Four members of the team of authors are grateful to the Simons Foundation Program: Presidential Discretionary-Ukraine Support Grants, Award №1030288.

We are grateful to the Armed Forces of Ukraine and all the defenders of Ukraine from Russian aggression, as well as the solidarity and support from many governments and individuals around the world, which makes our future work possible.

REFERENCES

1. G. Pintsuk et al. Materials for in-vessel components // *Fusion Engineering and Design.* 2022, p. 112994.
2. L. Malerba et al. Multiscale modelling for fusion and fission materials: The M4F project // *Nuclear Materials and Energy.* 2021, v. 29, p. 101051.
3. J.H. You et al. Limiters for DEMO wall protection: Initial design concepts & technology options // *Fusion Engineering and Design*. 2022, v. 174, p. 112988.
4. M. Wirtz et al. Transient heat load challenges for plasma-facing materials during long-term operation // *Nuclear Materials and Energy.* 2017, v. 12, p. 148-155.
5. N. Mantel et al. Development and testing of an additively manufactured lattice for DEMO limiters // *Nuclear Fusion.* 2022, v. 62, p**.** 036017.
6. M. Reinhart et al. Latest results of Eurofusion plasma-facing components research in the areas of power loading, material erosion and fuel retention // *Nuclear Fusion.* 2022, v. 62, p. 042013
7. J.W. Coenen et al. Evolution of Tungsten Fiber-Reinforced Tungsten-Remarks on Production and Joining // *Advanced Engineering Materials*. 2023, p. 2300569.

8. G. Marchese et al. Microstructural Evolution of Post-Processed Hastelloy X Alloy Fabricated by Laser Powder Bed Fusion // *Materials.* 2019, v. 12, p. 486.

9. O.V. Byrka et al. Modification and alloying effects in Eurofer steel under powerful pulsed plasma impacts // *Problems of Atomic Science and Technology*. *Series "Plasma Physics" (134).* 2021, N 4, p. 191-194.

10. R. Arredondo et al. Comparison experiment on the sputtering of EUROFER, RUSFER and CLAM steels by deuterium ions // *Nuclear Materials and Energy.* 2022, v. 30, p. 101118.

11. I.E. Garkusha et al. Materials surface damage and modification under high power plasma exposures // *Journal of Physics: Conference Series.* 2018, v. 959, p. 012004.

12. V.I. Tereshin et al. Pulsed plasma accelerators of different gas ions for surface modification // *Review of Scientific Instruments.* 2002, v. 73, p. 831.

13. V.A. Makhlai et al. Influence of surface tension on macroscopic erosion of castellated tungsten surfaces during repetitive transient plasma loads // *Nuclear Materials and Energy.* 2019, v. 19, p. 493-497.

14. V.A. Makhlaj et al. Dust generation mechanisms under powerful plasma impacts to the tungsten surfaces in ITER ELM simulation experiments // *Journal of Nuclear Materials.* 2013, v. 438, p. 233-236.

15. V.A. Makhlay et al. Effect of preheating on the damage to tungsten targets after repetitive ITER ELM-like heat loads // *Physica Scripta.* 2007, v. T128, p. 239-241.

16. I.E. Garkusha et al. Damage to preheated tungsten targets after multiple plasma impacts simulating ITER ELMs // *Journal of Nuclear Materials.* 2009, v. 386-388, p. 127-131.

17. I.E. Garkusha et al. High power plasma interaction with tungsten grades in ITER relevant conditions // *Journal of Physics: Conference Series.* 2015, v. 591, p. 012030.

18. V.A. Makhlai et al. High heat fluxes testing of tungsten materials with different microstructure under QSPA transient plasma impacts // *48th EPS Conference on Plasma Physics, EPS 2022*. 2022, Code 185044.

19. S.V. Malykhin et al. Mechanisms of crack generation in high-pure tungsten exposed to high power density plasma // *Nuclear Instruments and Methods in Physics Research Section B: Beam Interactions with Materials and Atoms*. 2020, v. 481, p. 6-11.

20. Lisong Zhang et al. Experimental and simulation studies on damage mechanisms of tungsten and molybdenum under compressed plasma flow irradiation // *Nuclear Fusion.* 2023, v. 63, p. 076010.

21. X. Liu et al. Morphological development of sub-grain cellular/bands microstructures in selective laser melting // *Materials.* 2019, v. 12, p. 1204.

22. J. Li et al. Preparation, microstructure, and microhardness of selective laser-melted W–3Ta sample // *Journal of Materials Research.* 2020, v. 35, p. 2016-2024.

23. Y. Hong et al. The cellular boundary with high density of dislocations governed the strengthening mechanism in selective laser melted 316L stainless steel *// Materials Science and Engineering A.* 2021, v. 799, p. 140279.

24. Y. Lee et al. Effect of Fluid Convection on Dendrite Arm Spacing in Laser Deposition // *Metallurgical and Materials Transactions B.* 2014, v. 45B, p. 1520-1529.

25. S.S. Herashchenko et al. Damaging of pure tungsten with different microstructure under sequential QSPA and LHD plasma loads // *Problems of Atomic Science and Technology*. *Series "Plasma Physics" (130).* 2020, N 6, p. 78-82.

26. V.A. Makhlaj et al. Residual stresses in tungsten under exposures with ITER ELM-like plasma loads // *Physica Scripta*. 2009, v. T138, p. 014060.

27. D.G. Solyakov et al. Formation of the compression zone in a plasma flow generated by a magnetoplasma compressor // *Plasma Physics Report.* 2011, v. 37, p. 948-954.

28. O.V. Byrka et al. Properties of modified surface layers of industrial steels samples processed by pulsed plasma streams // *Vacuum*. 2000, v. 58, p. 195-201.

29. D.V. Orlinski et al. First mirrors for diagnostic systems of an experimental fusion reactor I. Simulation mirror tests under neutron and ion bombardment // *Plasma Devices Operations.* 2007, v. 15, p. 33-75.

Article received 08.09.2023

ОСОБЛИВОСТІ МОДИФІКАЦІЙ У ПЕРЕЗАТВЕРДІЛИХ ПОВЕРХНЯХ ПЕРСПЕКТИВНИХ МАТЕРІАЛІВ ПІД ДІЄЮ ПОТУЖНИХ ПЛАЗМОВИХ ІМПУЛЬСІВ

С.С. Геращенко, В.О. Махлай, І.Є. Гаркуша, Ю.В. Петров, М.М. Аксьонов, М.В. Кулик, Д.В. Єлісєєв, П.Б. Шевчук, Ю.Є. Волкова, Т.М. Меренкова, M. Wirtz

Розглянуто модифікації поверхонь перспективних матеріалів за допомогою серії повторюваних плазмових імпульсів, які спричиняли плавлення вольфраму. Особливості пошкодженого шару референтних матеріалів (IGP W, AM W/WTa, Хастелой та EUROFER) ядерної та термоядерної енергетики досліджували після впливу плазми в установках (КСПП, МПК і ІПП) з різною тривалістю плазмових імпульсів. Детальний аналіз поверхні проводили за допомогою растрової електронної мікроскопії. Було виявлено, що плазмова обробка призвела до формування модифікованого шару в результаті швидкого повторного затвердіння експонованої поверхні. У перезатверділих шарах опромінених матеріалів з'явилися дрібноклітинні структури з типовими розмірами комірок близько 150…500 нм. Збільшення шорсткості експонованих поверхонь пояснювалося наявністю тріщин і повторно затверділого шару.